Crystallisation Kinetics of $Co_{75-x}M_xSi_{15}B_{10}$ (M = Fe, Mn, Cr and $x = 0$, 5) Amorphous Alloys

N. Bayri[a,*], V.S. Kolat[a], T. Izgi[a], S. Atalay[a], H. Gencer[a] and P. Sovak[b]

[a]Inonu University, Science and Arts Faculty, Physics Department, 44280 Malatya, Turkey

[b]P.J. Safarik University, Department of Physics, Kosice, Slovakia

(Received April 8, 2015; in final form November 11, 2015)

In this study, the effect of Fe, Mn and Cr substitution for Co on the crystallization kinetics of amorphous $Co_{75-x}M_xSi_{15}B_{10}$ (M = Fe, Mn and Cr; $x = 0$ and 5) alloys were investigated. The broad diffraction peaks in the X-ray diffraction patterns for as-quenched ribbons indicated that all of the samples exhibit an amorphous structure. The activation energies of the alloys were calculated from differential thermal analysis data using the Kissinger, Ozawa and Augis–Bennett models. The increased activation energy for Fe, Mn and Cr doped samples indicated that the thermal stability and the crystallization kinetics were improved in the doped samples. The value of the Avrami exponent indicated that the crystallization is typical diffusion controlled three-dimensional growth for all of the samples.

DOI: 10.12693/APhysPolA.129.84

PACS: 75.50.Kj, 65.40.–b, 68.55.A–

1. Introduction

In recent years, Co- and Fe-based amorphous alloys and their crystallization kinetics have been extensively studied due to their excellent physical and mechanical properties, such as high electrical resistivity, small eddy currents, high thermal stability, high corrosion resistance, outstanding mechanical properties, low fabrication cost, and soft magnetic properties along with the ease of machining due to the disordered structure [1–9]. These properties also lead to improvements in their electrical and corrosion properties. Soft magnetic materials are generally used in transformers, inductive devices, sensors and bioengineering applications [10]. Due to the above-mentioned excellent physical and mechanical properties, Co-based (Co–Si–B) amorphous and nanocrystalline alloys have been studied [11, 12]. It has been reported in many previous studies that crystallization kinetics and crystallization process are very important to understand properties of amorphous materials [11–17]. The study of the crystallization kinetics provides the activation energy (E_a) of the crystallization and the relevant parameters, such as the Avrami exponent (n) responsible for the mechanism of crystallization. Differential thermal analysis (DTA) has been used for such an investigation under both non-isothermal and isothermal conditions. The data obtained from non-isothermal crystallization have been analyzed using well-established theoretical models, namely the Kissinger [18], Ozawa [19] and Augis–Bennett [20] models. This analysis helps us to understand how metallic glasses crystallize.

While the influence of various substitute alloying elements on the crystallization kinetics of Fe- based amorphous alloys has been studied, there is a lack of studies regarding the crystallization kinetics of Co-based amorphous alloys. In this study, the influence of substitution of Co with Fe, Mn and Cr elements on the crystallization kinetics of $Co_{75-x}M_xSi_{15}B_{10}$ (M = Fe, Mn and Cr; $x = 0$ and 5) amorphous alloys was investigated in detail.

2. Experimental

Amorphous $Co_{75-x}M_xSi_{15}B_{10}$ (M = Fe, Mn and Cr; $x = 0$ and 5) ribbons were prepared via the melt-spinning technique. The crystallization behavior of the samples was investigated using DTA. Thermal data were measured at heating rates of 5, 10, 15 and 20 °C/min. The structure of the as-received samples was confirmed by X-ray powder diffraction (XRD) (Rigaku-Radb) measurements using Cu K_α (λ = 1.5405 Å) radiation. In the X-ray measurements, the power and scanning rate were set at 30 kV, 15 mA and 1°/min, respectively.

3. Results and discussion

Figure 1 shows the XRD patterns of the as-quenched $Co_{75-x}M_xSi_{15}B_{10}$ (M = Fe, Mn and Cr; $x = 0$ and 5) ribbons. The typical broad diffraction peaks in the XRD patterns for the as-quenched ribbons indicate that all of the alloys have amorphous structure.

Figure 2 shows the DTA curves for the as-quenched amorphous ribbons of $Co_{75-x}M_xSi_{15}B_{10}$ (M = Fe, Mn and Cr; $x = 0$ and 5) measured at a 10 °C/min heating rate in the temperature range of 400 to 700 °C. The first peak temperatures were observed at 506.6 °C for $Co_{75}Si_{15}B_{10}$, 518.1 °C for $Co_{70}Fe_5Si_{15}B_{10}$, 531.5 °C for $Co_{70}Mn_5Si_{15}B_{10}$ and 539.8 °C for $Co_{70}Cr_5Si_{15}B_{10}$ alloys. It is clear that the peak temperatures (T_p) increase with the addition of Fe, Mn and Cr. The addition of Fe, Mn and Cr to the $Co_{75}Si_{15}B_{10}$ base alloys slows the crystallization kinetics by increasing the thermal stability with

*corresponding author; e-mail: nevzat.bayri@inonu.edu.tr

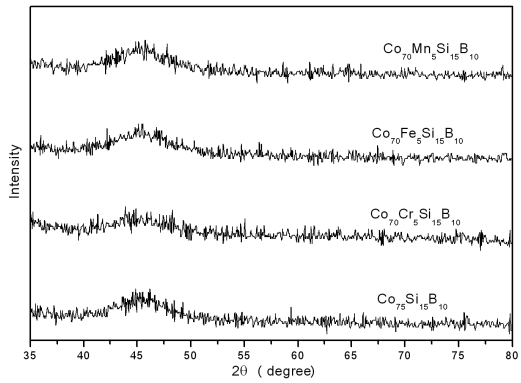

Fig. 1. XRD patterns of the as-quenched samples of $Co_{75-x}M_xSi_{15}B_{10}$ (M = Fe, Mn and Cr; $x = 0$ and 5).

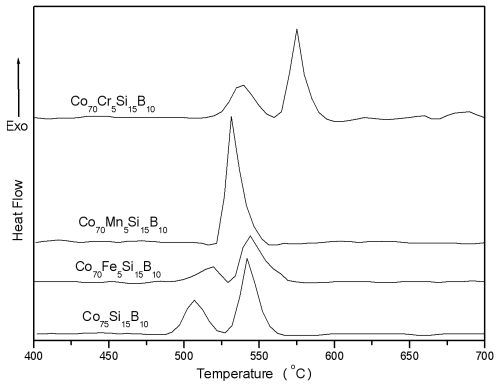

Fig. 2. DTA curves of the as-quenched amorphous alloys of $Co_{75-x}M_xSi_{15}B_{10}$ (M = Fe, Mn and Cr; $x = 0$ and 5) measured at a heating rate of 10 °C/min.

respect to crystallization. As can be seen from DTA measurements, although Mn substituted sample exhibits only one exothermic peak, the Fe and Cr substituted samples exhibit two distinct exothermic peaks. The presence of two exothermic peaks for Fe and Cr substituted samples could be interpreted as the formation of second crystallization phase and the crystallization process of the alloy proceeds through a multi-stage model [7, 11, 21].

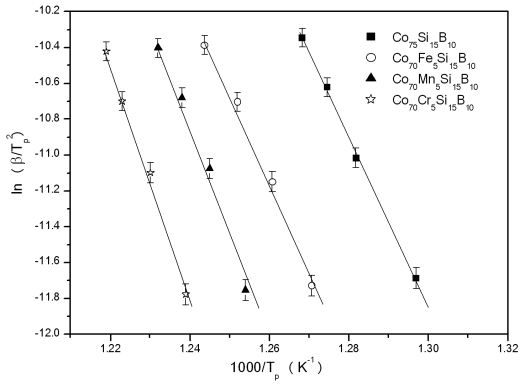

Fig. 3. Kissinger plot of the as-quenched amorphous ribbons of $Co_{75-x}M_xSi_{15}B_{10}$ (M = Fe, Mn and Cr; $x = 0$ and 5).

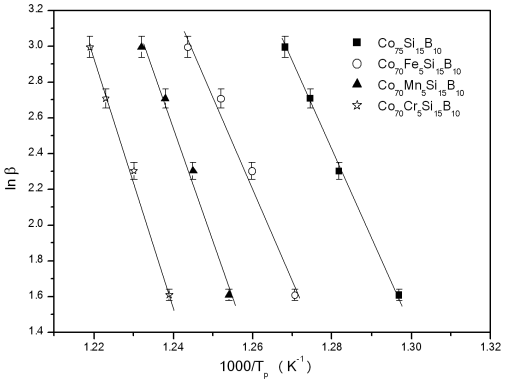

Fig. 4. Ozawa plot of the as-quenched amorphous ribbons of $Co_{75-x}M_xSi_{15}B_{10}$ (M = Fe, Mn and Cr; $x = 0$ and 5).

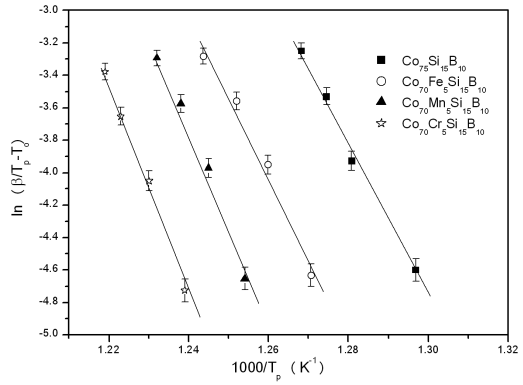

Fig. 5. Augis–Bennett plot of the as-quenched amorphous ribbons of $Co_{75-x}M_xSi_{15}B_{10}$ (M = Fe, Mn and Cr; $x = 0$ and 5).

The activation energy of the crystallization process gives important information regarding the thermal stability of the sample. The activation energies for the crystallization of the $Co_{75-x}M_xSi_{15}B_{10}$ (M = Fe, Mn and Cr; $x = 0$ and 5) alloys were determined from the DTA curves through the well-known Kissinger [18], Ozawa [19] and Augis–Bennett [20] equations, as given by Eqs. (1), (2), and (3), respectively

$$\ln\left(\frac{\beta}{T_{\mathrm{p}}^2}\right) = -\frac{E_{\mathrm{a}}}{RT_{\mathrm{p}}} + \text{const}, \tag{1}$$

$$\ln(\beta) = -\frac{E_{\mathrm{a}}}{RT_{\mathrm{p}}} + \text{const}, \tag{2}$$

$$\ln\left(\frac{\beta}{T_{\mathrm{p}} - T_0}\right) = -\frac{E_{\mathrm{a}}}{RT_{\mathrm{p}}} + const, \tag{3}$$

where β is the heating rate, T_{p} is the temperature at the exothermal peak, R is the gas constant, T_0 is the absolute temperature, and E_{a} is the activation energy of crystallization. The activation energies for the three models were calculated from the slopes of the plots of $\ln(\beta/T_{\mathrm{p}}^2)-1000/T_{\mathrm{p}}$, $\ln(\beta)-1000/T_{\mathrm{p}}$ and $\ln(\beta/T_{\mathrm{p}}-T_0)-1000/T_{\mathrm{p}}$, which yield approximately straight lines with good fits, as shown in Figs. 3–5, re-

spectively. Ozawa extended the Avrami equation to the non-isothermal condition. Assuming the maximum crystallization peak occurring at a crystallization fraction, this method involves the measurement of the temperature T from the experiments at different heating rates β. The Kissinger method assumes that the reaction rate is maximum at the peak temperature (T_p). This assumption also implies a constant degree of conversion at T_p. The Augis–Bennett method is an extension of the Kissinger method showing its applicability to heterogeneous reaction described by the Avrami expression. As can be seen, these three methods are very similar and require similar plots. The activation energies for the crystallization of the $Co_{75-x}M_xSi_{15}B_{10}$ (M = Fe, Mn and Cr; $x = 0$ and 5) alloys were determined by above mentioned three different methods in order to discuss the effectiveness of these three different methods.

TABLE I

Kinetic parameters (E_a [kJ/mol], n) of $Co_{75-x}M_xSi_{15}B_{10}$ (M = Fe, Mn and Cr; $x = 0$ and 5) amorphous alloys.

Alloy	Kissinger		Augis-Bennett		Ozawa		n
peak:	1	2	1	2	1	2	
$Co_{75}Si_{15}B_{10}$	391.35±3.9	470.54±4.7	394.21±7.9	475.17±9.5	404.30±12.1	485.36±14.6	2.52±0.05
$Co_{70}Fe_5Si_{15}B_{10}$	415.62±4.2	494.97±5	419.88±8.4	498.33±10	425.76±12.8	503.51±15.1	2.62±0.05
$Co_{70}Mn_5Si_{15}B_{10}$	511.65±5.1	–	514.90±10.3	–	525.06±15.7	–	2.18±0.04
$Co_{70}Cr_5Si_{15}B_{10}$	556.95±5.6	505.75±5.1	555.44±11.1	509.30±10.2	568.19±17	519.79±15.6	2.24±0.04

The activation energies calculated by three different methods are given in Table I. The values of the activation energies calculated from the Ozawa and Augis–Bennett equations are slightly higher than those from the Kissinger equation [13]. The comparison of activation energy determined from three different methods showed that the values are in good agreement with each other and also exhibit similar behavior. This means that one can use any of the three methods to calculate the activation energy. According to the Kissinger equation, the activation energies for the first peak were determined to be 391.35, 415.62, 511.65, 556.95 kJ/mol for the $Co_{75}Si_{15}B_{10}$, $Co_{70}Fe_5Si_{15}B_{10}$, $Co_{70}Mn_5Si_{15}B_{10}$ and $Co_{70}Cr_5Si_{15}B_{10}$ alloys, respectively. The activation energies calculated for second peaks also exhibited similar behavior.

The activation energy calculations indicated that the partial substitution of Fe, Mn, or Cr for Co in $Co_{75}Si_{15}B_{10}$ increases the activation energy. This result indicated that small amount of substitution elements produces a decreased rate of the crystallization kinetics. The largest values of activation energy for Mn and Cr doped samples compared with those of undoped and Fe doped samples were attributed to the relative size of the substitution elements. In previous studies, it has been concluded that the crystallization kinetics is closely related with relative size of substitution atoms [8, 22, 23]. The substitution elements of Fe (1.56 Å), Mn (1.61 Å) and Cr (1.66 Å) have a larger atomic size than Co (1.52 Å). The larger Mn and Cr atoms compared with Fe and Co enhance the potential barrier and hinder the diffusion of atoms in the crystallization process of amorphous alloys, and consequently, the activation energy increases for larger substitution atoms.

Generally, the crystallization kinetics of amorphous alloys are studied using the Johnson–Mehl–Avrami equation [16, 17], which is

$$x(t) = 1 - \exp(-(kt)^n), \tag{4}$$

where $x(t)$ is the fraction of the volume that has become crystalline at annealing time t, n is the Avrami parameter (related to nucleation and growth), and k is the reaction rate constant, which is a function of the absolute temperature and is given by the following equation:

$$k = k_0 \exp(-E_\mathrm{a}/RT), \tag{5}$$

where R is the gas constant, T is the absolute temperature, E_a is the activation energy, and k_0 is the frequency factor, which is a measure of the probability that a molecule with energy E_a will participate in a reaction. The method used to determine the Avrami parameter (n) was proposed by Ozawa [19]. During the DTA, the heating rates are controlled so that the temperature can be expressed as

$$T = T_0 + \beta T, \tag{6}$$

where T_0 is the initial temperature associated with the exothermic DTA peak. Combining Eqs. (4) and (6), we obtain

$$\left.\frac{\mathrm{d}\ln(-\ln(1-x))}{\mathrm{d}\ln\beta}\right|_T = -n. \tag{7}$$

The value of x at any selected T is calculated from the ratio of the partial area (S) of the crystallization peak at the selected T to the total area (S_0) of the crystallization exotherm. Equation (7) indicates that at any fixed temperature, the crystallization mechanism, or the Avrami exponent n, can be obtained from the slopes of the $\ln(-\ln(1-x)) - \ln(\beta)$ curves. The Avrami exponent n involves the information regarding the nucleation and growth mechanism in the crystallization process.

The calculated Avrami parameters (n) for the $Co_{75-x}M_xSi_{15}B_{10}$ (M = Fe, Mn and Cr; $x = 0$ and 5) alloys are listed in Table I. The Avrami equation and the derived exponent n are often used to obtain information on the transformation kinetics and the special dimensions of the growing crystals. The calculated values of n are 2.52, 2.62, 2.18 and 2.24 at the se-

lected temperatures of 515 °C for $Co_{75}Si_{15}B_{10}$, 520 °C for $Co_{70}Fe_5Si_{15}B_{10}$, 535 °C for $Co_{70}Mn_5Si_{15}B_{10}$ and 540 °C for $Co_{70}Cr_5Si_{15}B_{10}$, respectively. As presented in Table I, the values of n are not constant for the various doping elements, which imply that the nucleation and growth mechanism of the crystallization process are closely related with the doping elements. The calculated Avrami parameters, which are larger than 2.5 for $Co_{75}Si_{15}B_{10}$ and $Co_{70}Fe_5Si_{15}B_{10}$ alloys, indicates that the crystallization is governed by diffusion-controlled three-dimensional growth with a constant nucleation rate [13, 24, 25]. In addition, the smaller value of the Avrami parameters than 2.5 for $Co_{70}Mn_5Si_{15}B_{10}$ and $Co_{70}Cr_5Si_{15}B_{10}$ alloys could be interpreted as the crystallization is governed by three-dimensional growth with a decreasing nucleation rate [25].

4. Conclusions

In this study, the effect of Fe, Mn and Cr substitution for Co on the crystallization kinetics of amorphous $Co_{75-x}M_xSi_{15}B_{10}$ (M = Fe, Mn and Cr; $x = 0$ and 5) alloys was investigated. The activation energies of the alloys were calculated using the Kissinger, Ozawa and Augis–Bennett models based on differential thermal analysis data. The increased activation energies for Fe, Mn and Cr doped samples indicated that the thermal stability and the crystallization kinetics were improved in the doped samples. Among the doping atoms, Cr was determined to have the highest thermal stability. The Avrami exponent n was calculated from the Johnson–Mehl–Avrami equation. The Avrami parameters of $Co_{75-x}M_xSi_{15}B_{10}$ (M = Fe, Mn and Cr; $x = 0$ and 5) alloys varies in the range of $2 < n < 3$. The value of the Avrami exponent indicated that the crystallization is typical diffusion controlled three-dimensional growth for all of the samples. The nucleation rate is constant for $Co_{75}Si_{15}B_{10}$ and $Co_{70}Fe_5Si_{15}B_{10}$, while a decreasing nucleation rate was observed for $Co_{70}Mn_5Si_{15}B_{10}$ and $Co_{70}Cr_5Si_{15}B_{10}$ samples.

Acknowledgments

This work was supported by Inonu University, project number 2012/37.

References

[1] N. Chau, N.H. Luong, N.X. Chien, P.Q. Thanh, L.V. Vu, *Physica B* **327**, 241 (2003).

[2] J.S. Blazquez, J.M. Borrego, C.F. Conde, A. Conde, J.M. Grenche, *J. Phys. Condens. Matter* **15**, 3957 (2003).

[3] H. Wu, Y. Liu, S.W. He, Z.M. Liu, B.Y. Nuang, *Int. J. Mater. Res.* **99**, 689 (2008).

[4] C. Gomez-Polo, J.I. Perez-Landazabal, V. Recarte, *IEEE Trans. Magn.* **39**, 3019 (2003).

[5] N. Chau, N.Q. Hoa, N.H. Luong, *J. Magn. Magn. Mater.* **290**, 1547 (2005).

[6] N.Q. Hoa, N. Chau, S.C. Yu, T.M. Thang, N.D. The, N.D. Tho, *Mater. Sci. Eng. A* **449**, 364 (2007).

[7] A.K. Panda, S. Kumari, I. Chattora, P. Svec, A. Mitra, *Philos. Mag.* **85**, 1835 (2005).

[8] H. Gencer, T. Izgi, V.S. Kolat, N. Bayri, S. Atalay, *J. Non-Cryst. Solids* **379**, 185 (2013).

[9] S. Atalay, H. Gencer, A.O. Kaya, V.S. Kolat, T. Izgi, *J. Non-Cryst. Solids* **365**, 99 (2013).

[10] M.E. McHenry, M.A. Willard, D.E. Laughlin, *Prog. Mater. Sci.* **44**, 291 (1999).

[11] M. Millan, J.S. Blazquez, C.F. Conde, A. Conde, S. Lozano-Perez, P. Ochin, *J. Non-Cryst. Solids* **355**, 109 (2009).

[12] R. Andrejco, P. Vojtanik, *J. Magn. Magn. Mater.* **280**, 108 (2004).

[13] N. Bayri, T. Izgi, H. Gencer, P. Sovak, M. Gunes, S. Atalay, *J. Non-Cryst. Solids* **355**, 12 (2009).

[14] S.M. Hoque, A.K.M.R. Haque, Md. Obaidur Rahman, N.H. Nghi, M.A. Hakim, S. Akhter, *J. Non-Cryst. Solids* **357**, 2109 (2011).

[15] M. Gomez, A. Rosales-Rivera, P. Pineda-Gomez, D. Muraca, H. Sirkin, *Microelectron. J.* **39**, 1242 (2008).

[16] W.A. Johnson, R.F. Mehl, *Trans. Am. Inst. Min. Eng.* **135**, 416 (1939).

[17] M. Avrami, *J. Chem. Phys.* **9**, 177 (1941).

[18] H.E. Kissinger, *J. Res. NBS* **57**, 217 (1956).

[19] T. Ozawa, *Bull. Chem. Soc. Jpn.* **35**, 1881 (1965).

[20] J.A. Augis, J.E. Bennett, *J. Therm. Anal.* **13**, 283 (1978).

[21] D.M. Minic, A.M. Maricic, R.Z. Dimitrijevic, M.M. Ristic, *J. Alloys Comp.* **430**, 241 (2007).

[22] Z. Jamili-Shirvan, M. Haddad-Sabzevar, *J. Ultrafine Grained and Nanostruct. Mater.* **16**, 55 (2013).

[23] F.Q. Zhai, E. Pineda, M.J. Duarte, D. Cresp, *J. Alloys Comp.* **604**, 157 (2014).

[24] J. Malek, *Thermochim. Acta* **267**, 61 (1995).

[25] X. Wang, D. Wang, B. Zhu, Y. Li, F. Han, *J. Non-Cryst. Solids* **385**, 111 (2014).